Journal of Casting & Materials Engineering Vol. 6 No. 3 (2022) 64–68
https://doi.org/10.7494/jcme.2022.6.3.64

The Effect of High Silicon and Molybdenum Content on the Mechanical Properties and Microstructure of Gray Cast Iron

Łukasz Dyrlaga[a, b,*], Dariusz Kopyciński[a], Edward Guzik[a], Grzegorz Soból[a], Dariusz Borak[b]

[a]AGH Univestity of Science and Technology, Faculty of Foundry Engineering, Reymonta 23 St., 30 059 Krakow, Poland
[b]METALPOL Węgierska Górka sp. z o.o., ul. Kolejowa 6, 34-350 Węgierska Górka, Poland
**e-mail: dyrlaga@agh.edu.pl*

Received: 7 February 2022/Accepted: 30 September 2022/Published online: 1 October 2022.
This article is published with open access at AGH University of Science and Technology Journals.

Abstract

This paper presents an overview of the current knowledge concerning SiMo ductile cast iron begins by describing the standard type of ductile cast iron before proceding to description of its microstructures. The paper then presents its chemical composition and the significant influence of individual elements on technological and mechanical properties. The research section focuses the influence of the addition of Si and Mo to the matrix of gray iron. After casting, stepped samples were carried out on the microstructure along with UTS tensile strength tests. The research presented in the article is a preliminary step towards the goal of obtaining a stable production process for silico-molybdenum cast iron.

Keywords:

SiMo cast iron, structure, mechanical properties, chemical composition, gray iron

1. INTRODUCTION

Increasingly, iron castings are required to withstand high temperatures, a phenomenon particularly visible in the production and operation of internal combustion vehicles. In this case, two types of loads can be distinguished that act on the cast parts of exhaust systems. The first is thermal loads and the second is thermochemical [1]. In addition, thermal loads can have a static effect on cast iron (heating up to a certain treatment temperature and withstanding it) and transiently (alternately heating and cooling machine parts) [2]. Modern internal combustion cars, in order to achieve the highest possible performance while reducing pollutants introduced into the atmosphere, are most often designed with turbines and exhaust gas collectors, and thus the temperature during operation can even reach over 1000°C [3]. Moreover, the casting itself may heat up unevenly during operation, which in turn leads to internal stresses [4]. In the production of machine parts exposed to these thermal loads SiMo ductile cast iron can be used, which retains the positive technological properties of classic nodular cast iron, while at the same time enjoying high thermal resistance [5]. The review of the current knowledge will allow the development of a technology for the production of SiMo cast iron castings in production conditions, as well as to adjust the process parameters in order to obtain a finished product of the highest quality. Factors such as chemical composition, the iron melting process, nodularization and inoculation should all be taken into account. In this paper we focus on the influence of increased content of silicon and molybdenum on the functional properties of gray cast iron to prevent the growth of unfavorable primary graphites [6]. As there is no mention of this type of cast iron in the literature, but only the corrosion resistance of high-silicon gray cast iron, the knowledge about SiMo ductile cast iron will serve as theoretical basis.

1.1. Grades and structure of SiMo ductile iron

SiMo cast iron grades were included in the EN 16124 standard. There are 9 grades of cast iron which, together with the silicon and molybdenum contents and the basic mechanical parameters, are presented in Table 1.

Molybdenum at higher contents causes perlite to appear in the matrix and this is not conducive to obtaining the appropriate mechanical properties. At 0.8% molybdenum, perlite with carbides appears between the ferrite grains [7].

Table 1
Symbols, chemical composition, and basic mechanical properties of SiMo ductile cast iron, based on [8]

Symbol	Chemical composition [%]		Tensile strength [MPa min.]	0.2% proof strength [MPa min.]	Elongation [% min.]	Brinell hardness
	Silicon	Molybdenum				HBW [1]
EN-GJS-SiMo25-5	2.3–2.7	0.4–0.6	420 [2]	260 [2]	12	140–210 [2]
			400 [3]	250 [3]		130–200 [3]
EN-GJS-SiMo30-7	2.8–3.2	0.6–0.8	440 [2]	310 [2]	10	150–220 [2]
			420 [3]	300 [3]		140–210 [3]
EN-GJS-SiMo35-5	3.3–3.7	0.4–0.6	440 [2]	330 [2]	8	160–230 [2]
			440 [3]	320 [3]		150–220 [3]
EN-GJS-SiMo40-6	3.8–4.2	0.5–0.7	480	380	8	190–240
EN-GJS-SiMo40-10		0.8–1.1	510	400	6	190–240
EN-GJS-SiMo45-6	4.3–4.7	0.5–0.7	520	420	7	200–250
EN-GJS-SiMo45-10		0.8–1.1	550	460	5	200–250
EN-GJS-SiMo50-6	4.8–5.2	0.5–0.7	580	480	4	210–260
EN-GJS-SiMo50-10		0.8–1.1	600	500	3	210–260

1) Approximate values, measurement on castings.
2) For the wall thickness g [mm]; $30 < g \leq 60$.
3) For the wall thickness g [mm]; $60 < g \leq 200$.

The 0.94% molybdenum content favors the formation of a larger amount of pearlite in the matrix. In the first case, the amount of silicon is 3.6% and in the second, 4.1%. The amount of manganese is 0.15% in the first one, and 0.38 in the second [9, 10].

The high molybdenum content increases the chances of unfavorable M_6C and M_7C_3 carbides at the grain boundaries. The heat treatment applied to SiMo iron castings is able to eliminate secondary carbides and pearlite, leading to the ferritization of the matrix. As can be seen from the phase diagram, M_7C_3 carbides are only stable down to a temperature of less than about 300°C. After heat treatment, ferrite saturated with molybdenum emits fine dispersion carbides in its grains and not at the grain boundaries, which has a positive effect on the mechanical properties. This heat treatment does not work with M_6C primary carbides which are stable and only dissolve above about 1100°C [9].

1.2. Mechanical properties and influence of Mo, Si, Al, and Cr

SiMo ductile iron castings must exhibit increased mechanical properties at high temperatures and the addition of molybdenum increases the temperature range of such castings. Molybdenum also increases the tensile strength UTS of SiMo cast iron. It is an element that increase the amount of pearlite in the matrix, which, at higher contents (about 1% mas.), may have an unfavorable effect on the structure. As mentioned earlier, precipitation of pearlite at the grain boundaries decreases the tensile strength and ductility and a heat treatment to obtain ferrite in the matrix may be necessary. The high content of silicon in this type of cast iron partially neutralizes the harmful effect of molybdenum on the structure and properties, increasing the ability to ferrite cast iron. As a result, the elongation increases. Due to its properties, silicon causes that the amount of carbon in cast iron in foundry practice does not exceed 3% mass, especially with contents above 4.5% Si mas. [11–14].

The research [12] showed that cast iron with the addition of 4.0% Si and 1.4% Mo has good mechanical properties at a temperature of up to 600°C.

Chromium as an additive to cast iron increases resistance to high temperature [15]. As a component of nickel-chromium cast iron in the amount of up to 2%, it also has a positive effect on hardness [16]. Chromium amplifies the tendency of cast iron to metastable crystallization with precipitates of carbides, which may necessitate the production of cast iron with the addition of aluminum.

Aluminum improves the graphitization of cast iron. With an aluminum content of 3.2–3.8%, the matrix is ferritic. Such an increase in the ferritization capacity of cast iron can help to obtain the appropriate structure of SiMo cast iron while increasing its resistance to high temperatures [15, 17–19].

2. RESEARCH METHODOLOGY

The initial cast iron was melted twice in a medium-frequency induction furnace with a chamotte-graphite crucible with a capacity of 15 kg, which is provided by the Experimental Foundry of the Faculty of Foundry Engineering, AGH University of Science and Technology. At the end of each melt, the liquid cast iron was superheated to a temperature of 1490–1500 °C and this was maintained for a period of 3 minutes. The procedure of inoculation liquid metal was performed by introducing a zirconium inoculant with a granulation from 2 to 5 mm, by Elkem. The material had been selected to prepare ductile iron castings with an increased content of silicon and molybdenum. Nodularization treatment was prepared by means of the bell method using a blend containing 17% magnesium. A stepped sample (Fig. 1. and Fig. 2.), and a sample for chemical composition has been cast of each melt. The chemical composition was checked ona Bruker spectrometer. Metallographic, and tensile strength samples were cut from the prepared castings (Fig. 3.).

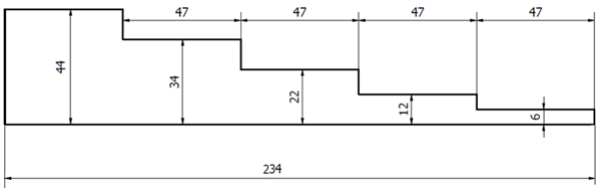

Fig. 1. Research sample dimensions

Fig. 2. Research samples of cast iron

Fig. 3. Gray iron tensile strength sample made according to the customer's standard. Diameter of the sample D = 6 mm, length without fixings L = 15 mm

3. RESULTS

The chemical composition of the cast samples is shown in Table 2. Sample 1 and 2 were made of the same heat, while sample 3 was at another heat. In both cases, the bell spheroidization was attempted, but due to the high concentration of magnesium in the spheroidizer (17%), the attempt was unsuccessful. Further research mainly concerns mainly the matrix and carbide precipitates.

Table 2
Chemical compositions of obtained cast irons

Sample number	Content [%]								
	C	Si	Mo	Mn	Cr	S	Al	Cu	Mg
1 2	2.44	5.67	0.77	0.42	0.08	0.01	0.01	0.12	<0.015
3	2.62	5.54	0.79	0.39	0.09	0.018	0.01	0.09	<0.015

The results of the tensile strength UTS tests are presented in Table 3. The lack of the elongation parameter is caused by the overly small size of the sample and the inability to install an extensometer.

Table 3
Tensile strength of obtained cast irons

Sample number	Step number	Wall thickness [mm]	R_m [MPa]
1	2	12	325
	3	22	297
2	2	12	306
	3	22	261
3	2	12	203
	3	22	162

The microstructure of each sample is shown in Figure 4. All photos are taken at 100× magnification. The pictures of non-etched structures clearly show that it is gray cast iron. We are dealing here with the predominant amount of type A flake graphite. In the wall thickness of 34 mm, it is especially noticeable that there are also type C graphite precipitates in the microstructure.

After etching the structures with nitrile, it can be seen that the cast iron matrix is practically pure ferrite. Pearlite appears at the grain boundaries, but there is not much of it. The greatest amount of pearlite at the grain boundaries is found in sample 3. Moreover, the precipitates of flake graphite in this sample are the largest and their amount is the highest.

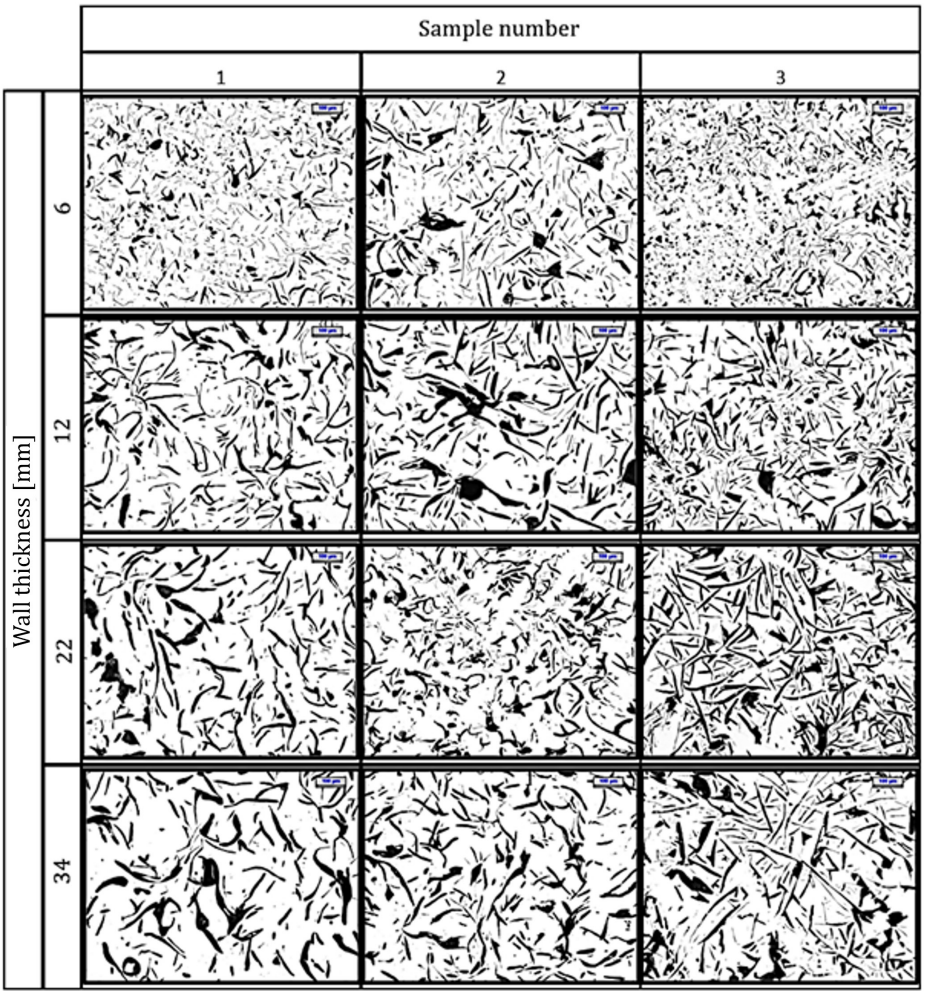

Fig. 4. Microstructures of prepared samples, non-etched, magnification 100×

This mainly applies to thicker walls, since sample 3 has very fine graphites on the 6 mm wall. Only M_6C primary carbides can be seen at the grain boundaries. The etched structure is shown in Figure 5.

Sample 2 has an evenly distributed graphite and their size is more uniform than in samples 1 and 3. The graphite precipitates themselves are less than in sample 3, instead carbide clusters were found. In this sample, precipitation of M_6C carbides and small amounts of M_7C_3 carbides can be seen as shown in Figure 6.

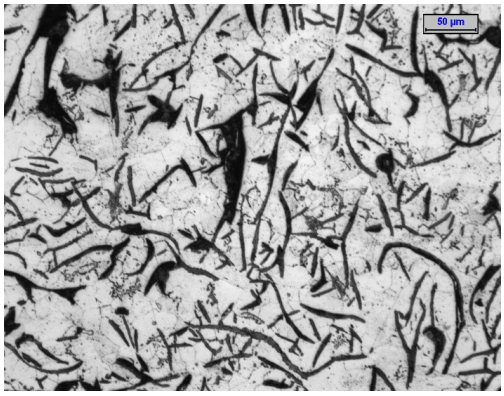

Fig. 5. Microstructures sample 3 in 22 mm wall thickness. Etched, magnification 200×

a)

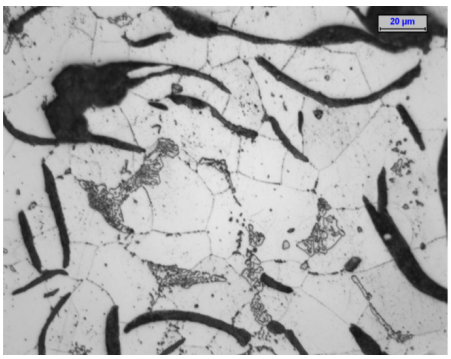

b)

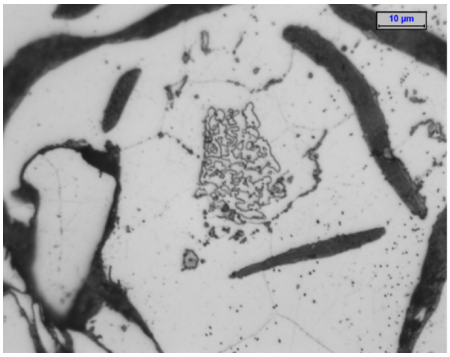

Fig. 6. Precipitations of M6C carbides at the grain boundaries of sample 2 in 22 mm wall thickness. Etched, magnification 500× (a) and 1000× (b)

Sample 1 has the least amount of pearlite at the grain boundaries, while there are large clusters of carbide precipitates. Here, the largest amount of M_7C_3 carbides occurs, but the vast majority of carbide precipitates are M_6C. An exemplary structure at a magnification of 500× is shown in Figure 7.

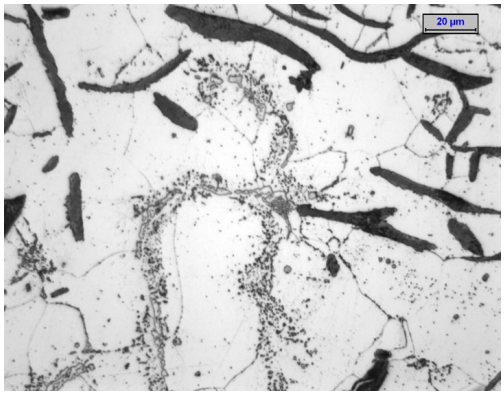

Fig. 7. Precipitations of M_6C and M_7C_3 carbides at the grain boundaries of sample 1, 34 mm wall thickness. Etched, magnification 500×

4. CONCLUSIONS

By analyzing the research results, the following conclusions can be drawn:

- Spheroidization with a 17% Mg blend is a bad solution in such a small crucible. Subsequent treatments will be performed with an alloy containing no more than 6% Mg.
- It is possible to obtain a gray cast iron structure with an increased content of silicon and molybdenum with the presence of M_6C and M_7C_3 carbides.
- Samples with finer particles of graphite in their structure (samples 1 and 2) are characterized by higher strength properties (UTS).
- Due to the absence of nodular graphite in the structure, cast iron has a much lower tensile strength than expected.
- The higher carbon content with the simultaneous high silicon content in sample 3 resulted in the formation of a large amount of flake graphite particles, which weakened the structure, leading to lower mechanical properties.
- The obtained cast iron could be an interesting alternative to cast iron used for castings of brake discs and pads, if good anti-abrasive and anti-corrosion properties are confirmed.
- In subsequent tests, heat treatment of the obtained samples should be carried out in order to try to eliminate large precipitates of carbides at the grain boundaries.

REFERENCES

[1] Lekakh S.N., Buchely M., O'Malley R., Godlewski L. & Mei Li. (2021). Thermo-cycling fatigue of SiMo ductile iron using a modified thermo-mechanical test. *International Journal of Fatigue*, 148, 106218. Doi: https://doi.org/10.1016/j.ijfatigue.2021.106218.

[2] Castro Güiza G.M., Hormaza W., Galvis E.A.R. & Mïndez Moreno L.M. (2017). Bending overload and thermal fatigue fractures in a cast exhaust manifold. *Engineering Failure Analysis*, 82, 138–148. Doi: https://doi.org/10.1016/j.engfailanal.2017.08.016.

[3] Karnik A.Y. & Shelby M.H. (2010). Effect of Exhaust Gas Temperature Limits on the Peak Power Performance of a Turbocharged Gasoline Engine. *Journal of Engineering for Gas Turbines and Power*, 132(11), 112801. Doi: https://doi.org/10.1115/1.4000856.

[4] Rathnaraj D.J. (2012). Thermomechanical fatigue analysis of stainless steel exhaust manifolds. *International Journal of Engineering, Science and Technology*, 2(2), 265.

[5] Black B., Burger G., Logan R., Perrin R. & Gundlach R. (2002). Microstructure and Dimensional Stability in Si-Mo Ductile Irons for Elevated Temperature Applications. *SAE Technical Paper*. 2002-01-2115. Doi: https://doi.org/10.4271/2002-01-2115.

[6] Dorula J., Kopyciński D., Guzik E., Szczęsny A. & Gurgul D. (2021). The Influence of Undercooling ΔT on the Structure and Tensile Strength of Gray Cast Iron. *Materials*, 14(21), 6682. Doi: https://doi.org/10.3390/ma14216682.

[7] Dawi K., Favergeon J. & Moulin G. (2008). High Temperature Corrosion of the Si-Mo Cast Iron in Exhaust Atmosphere. *Materials Science Forum*, 595–598, 743–751. Doi: https://doi.org/10.4028/www.scientific.net/msf.595-598.743.

[8] Standard EN 16124:2012. Founding – Low-alloyed ferritic spheroidal graphite cast irons for elevated temperature applications.

[9] Çelik G.A., Tzini M.-I.T., Polat Ş. Aristeidakis J.S., Atapek Ş.H., Sarafoglou P.I. & Haidemenopoulos G.N. (2021). Simulation and analysis of the solidification characteristics of a Si-Mo ductile iron. *Journal of Mining and Metallurgy Section B: Metallurgy*, 57(1), 53–62. Doi: https://doi.org/10.2298/JMMB200717003C.

[10] Vaško A. (2020). Comparison of mechanical and fatigue properties of SiMo- and SiCu-types of nodular cast iron. *Materialstoday: Proceedings*, 32(2), 168–173. Doi: https://doi.org/10.1016/j.matpr.2020.04.184.

[11] Åberg L.M. & Hartung C. (2012). Solidification of SiMo Nodular Cast Iron for High Temperature Applications. Indian Institute of Metals. *Transactions of the Indian Institute of Metals*, 65(6), 633–636. Doi: https://doi.org/10.1007/s12666-012-0216-8.

[12] Matteis P., Scavino G., Castello A. & Firrao D. (2014). High temperature fatigue properties of Si-Mo Ductile Cast iron. *Procedia Materials Science*, 3, 2154–2159. Doi: https://doi.org/10.1016/j.mspro.2014.06.349.

[13] Górny M., Kawalec M., Gracz B. & Tupaj M. (2021). Influence of Cooling Rate on Microstructure Formation of Si-Mo Ductile Iron Castings. *Metals*, 11(10), 1634. Doi: https://doi.org/10.3390/met11101634.

[14] Angella G., Taloni M., Donnini R. & Zanardi F. (2022). The Correlation between Solidification Rates, Microstructure Integrity and Tensile Plastic Behaviour in 4.2 wt.% Silicon Strengthened Ductile Iron. *Journal of Casting & Materials Engineering*, 6(1), 1–8. Doi: https://doi.org/10.7494/jcme.2022.6.1.1.

[15] Dyrlaga Ł., Kopyciński D., Guzik E. & Szczęsny A. (2021). Struktura i właściwości żeliwa odpornego na działanie wysokiej temperatury oraz na zużycie ścierne. In: J.J. Sobczak (red.), *Metalurgia 2020*, 326–343.

[16] Mourad M., El-Hadad S. & Ibrahim M.M. (2015). Effects of Molybdenum Addition on the Microstructure and Mechanical Properties of Ni-Hard White Cast Iron. *Transactions of the Indian Institute of Metals*, 68, 715–722. Doi: https://doi.org/10.1007/s12666-014-0504-6.

[17] Kashani S.M. & Boutorabi S.M.A. (2009). As-Cast Acicular Ductile Aluminum Cast Iron. *Journal of Iron and Steel Research International*, 16(6), 23–28. Doi: https://doi.org/10.1016/S1006-706X(10)60022-2.

[18] Gilewski R., Kopyciński D., Guzik E. & Szczęsny A. (2021). An Evaluation of the Microstructure of High-Aluminum Cast Iron in Terms of the Replacement of Aluminum Carbide with Titanium Carbide or Tungsten Carbide. *Applied Sciences,* 11(20), 9527. Doi: https://doi.org/10.3390/app11209527.

[19] Gilewski R., Kopyciński D., Guzik E. & Szczęsny A. (2021). Shaping the Microstructure of High-Aluminum Cast Iron in Terms of the Phenomenon of Spontaneous Decomposition Generated by the Presence of Aluminum Carbide. *Materials*, 14(20), 5993. Doi: https://doi.org/10.3390/ma14205993.